

Ultra High Energy Cosmic Rays: The disappointing model

R. Aloisio^a, V. Berezhinsky^{a,b}, A. Gazizov^{b,c,*}

^a*INFN, National Gran Sasso Laboratory, I-67010 Assergi (AQ), Italy*

^b*Gran Sasso Astroparticle Center, I-67010 Assergi (AQ), Italy*

^c*B.I. Stepanov Institute of Physics of NASB, 68 Independence Avenue, BY-22072 Minsk, Belarus*

Abstract

We develop a model for explaining the data of Pierre Auger Observatory (Auger) for Ultra High Energy Cosmic Rays (UHECR), in particular, the mass composition being steadily heavier with increasing energy from 3 EeV to 35 EeV. The model is based on the proton-dominated composition in the energy range (1 - 3) EeV observed in both Auger and HiRes experiments. Assuming extragalactic origin of this component, we argue that it must disappear at higher energies due to a low maximum energy of acceleration, $E_p^{\max} \sim (4 - 10)$ EeV. Under an assumption of rigidity acceleration mechanism, the maximum acceleration energy for a nucleus with the charge number Z is ZE_p^{\max} , and the highest energy in the spectrum, reached by Iron, does not exceed (100 - 200) EeV. The growth of atomic weight with energy, observed in Auger, is provided by the rigidity mechanism of acceleration, since at each energy $E = ZE_p^{\max}$ the contribution of nuclei with $Z' < Z$ vanishes. The described model has disappointing consequences for future observations in UHECR: Since average energies per nucleon for all nuclei are less than (2-4) EeV, (i) pion photo-production on CMB photons in extragalactic space is absent; (ii) GZK cutoff in the spectrum does not exist; (iii) cosmogenic neutrinos produced on CMBR are absent; (iv) fluxes of cosmogenic neutrinos produced on infrared - optical background radiation are too low for registration by existing detectors and projects. Due to nuclei deflection in galactic magnetic fields, the correlation with nearby sources is absent even at highest energies.

Keywords: ultrahigh energy cosmic rays, cosmic ray theory, cosmic ray experiment

PACS: 95.85.Ry, 96.40.-z, 95.85.Ry, 98.70.Sa

1. Introduction

There is a dramatic conflict between recent observational data of two largest UHECR detectors: HiRes [1] and Auger [2]. The HiRes data confirm well signatures of *proton* propagation through cosmic microwave background radiation (CMBR), the GZK cutoff [3, 4] and the pair-production dip [5, 6, 7, 8, 9], together with a proton-dominated mass composition [10, 11]. The Auger data strongly favor the nuclei composition getting progressively heavier in an energy range (4 - 40) EeV and indicate a strong spectrum steepening at highest energies not much consistent with the predicted shape of the GZK cutoff.

Preliminary results of the new Telescope Array experiment [12, 13] are in good agreement with the HiRes data both in spectrum, chemical composition and in the observed isotropy of UHECR arrival directions.

We shall discuss first the HiRes data. In the left panel of Fig. 1 the comparison of the HiRes data with the calculated pair-production dip and the GZK cutoff is shown in terms of modification factor $\eta(E)$. This quantity is given by a ratio of the energy spectrum $J_p(E)$ calculated with all energy losses taken into account, and the unmodified spectrum J_p^{unm} , where only adiabatic energy loss (the red-shift) is included: $\eta(E) = J_p(E)/J_p^{\text{unm}}(E)$. The modification factor is a convenient quantity, describing the dip and the beginning of the GZK cutoff practically model-independent way (see [6, 7]). These two spectral features are

*Corresponding author

Email address: askhat.gazizov@lngs.infn.it (A. Gazizov)

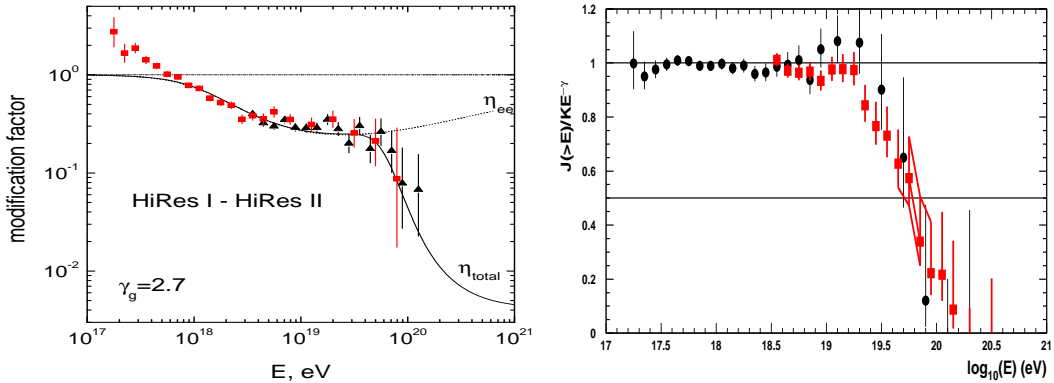


Figure 1: *Left panel:* Pair-production dip and GZK cutoff in terms of modification factor in comparison with the HiRes observational data [1] (HiRes 2 monocular – boxes, HiRes 1 monocular – triangles). Curves η_{tot} and η_{ee} show the total spectrum and the spectrum calculated with only adiabatic and pair-production energy losses included, respectively. *Right panel:* $E_{1/2}$ as a numerical characteristic of the GZK cutoff in the integral HiRes spectrum (see text); HiRes 2 monocular – circles, HiRes 1 monocular – boxes.

the signatures of protons interacting with CMBR. In the left panel of Fig. 1 one can see the good agreement of the HiRes spectrum with both dip and the GZK cutoff. The nature of the spectrum steepening seen in Fig. 1 as the GZK cutoff is further confirmed by the right panel of Fig. 1 valid for the integral spectrum.

In the integral spectrum the GZK cutoff is characterized by the energy $E_{1/2}$, where the calculated spectrum $J(>E)$ becomes half of the power-law extrapolation spectrum $KE^{-\gamma}$ from low energies. As calculations [5] show, this energy is $E_{1/2} = 10^{19.72}$ eV for a wide range of generation indices from 2.1 to 2.8. HiRes collaboration found $E_{1/2} = 10^{19.73 \pm 0.07}$ eV in a good agreement with the theoretical prediction. In the right panel of Fig. 1 we reproduce the HiRes graph [1] from which $E_{1/2}$ was determined. The plotted value is given by ratio of the measured flux $J(>E)$ and its power-law approximation $KE^{-\gamma}$. An extrapolation of this ratio to higher energies is given by 1 (unity), while the intersection of the measured ratio with the horizontal line 1/2 gives $E_{1/2}$.

With some caution one may conclude that HiRes has detected the signatures of proton interaction with CMBR in the form of pair-production dip and GZK cutoff. The final proof of this conclusion must come from the direct measurement of the mass composition of primaries.

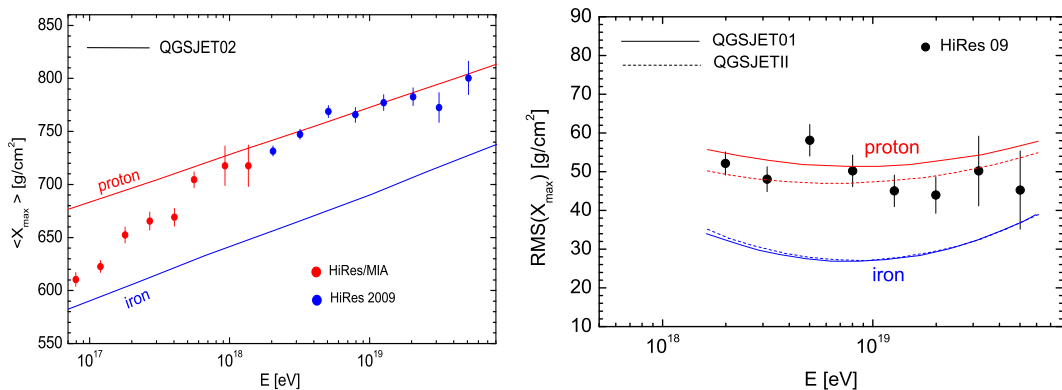


Figure 2: X_{max} as function of energy (*left panel*) and $RMS(X_{max})$, the width of distribution over X_{max} , (*right panel*) from HiRes data [10, 11]. The calculated values for protons and Iron are given according to QGSJETII model [14]. Note that the theoretical curves for RMS in the right panel have different shape than in the right panel of Fig. 3. It is caused by using in the HiRes analysis the truncated Gaussian distribution over X_{max} [10, 15, 16], while the Auger collaboration does not introduce any cuts.

The HiRes measurements of elongation rate and distribution over X_{\max} , the atmospheric height of the shower maximum, confirm the dominance of proton composition, indeed. In Fig. 2 we plot the data of HiRes [10, 11] on X_{\max} as a function of energy (elongation curve) and $\text{RMS}(X_{\max})$, the width of distribution over X_{\max} . One can see that both quantities agree with proton-dominated composition.

The Auger data on spectra and mass composition are quite different. In contrast to HiRes, the Auger data [17, 18, 19] show nuclei mass composition starting at $E \sim 4$ EeV, which becomes progressively heavier as energy increases (see Fig. 3). The change of the mass composition with energy is quite smooth, probably only with one peak at $E \approx 7$ EeV. It may indicate that the charge number Z changes smoothly in sources. The energy spectrum has a sharp steepening at $E \sim (30 - 40)$ EeV (see squares in Fig. 4), but energy shape of this steepening, as our calculations show, is quite different from the one predicted for the GZK cutoff. This is not surprising taking into account the Auger mass composition.

The width of the X_{\max} distribution is a very powerful tool for determination of the UHECR mass composition [20]. It is free of many uncertainties involved in the X_{\max} absolute value measuring method; the narrow width found in Auger experiment is difficult to falsify. On the other hand, the whole picture obtained by HiRes looks self-consistent. In particular, the confirmation of the pair-production dip in four experiments, including the early Auger data [6, 7, 8, 9], is a strong experimental argument in favor of the proton-dominated composition. The sources in this case can be AGN [8] with a neutron mechanism of exit [21, 22, 23].

In this paper we concentrate on the consequences from the mass composition and energy spectrum measured *only* by the Auger detector and look for a natural model explaining these data.

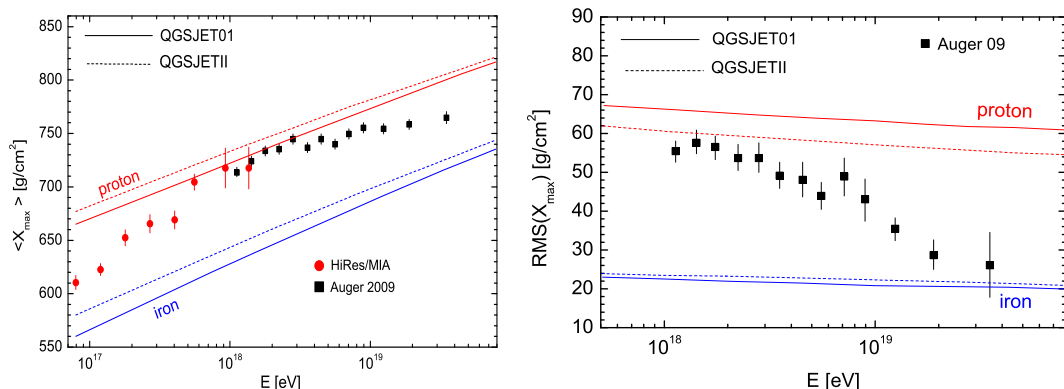


Figure 3: Auger data [17, 18, 19] on X_{\max} as a function of energy (left panel) and on $\text{RMS}(X_{\max})$, the width of distribution over X_{\max} , (right panel). The calculated values for protons and Iron are given according to QGSJETII model [14]. One can see from the right panel that RMS distribution becomes more narrow with energy increasing which implies the heavier composition.

2. Assumptions and features of the model

We consider a physical model directly following from the Auger observations with some additional ingredients. The accepted assumptions will be justified in the end of this section.

The basic assumption in our model is the proton composition in the energy range $(1 - 3)$ EeV, which is supported by observations of both detectors Auger and HiRes (see Fig. 3, especially the left panel for the Auger data and Fig. 2 for the HiRes data). We combine this observation with an additional assumption that these protons are extragalactic. The third ingredient of our model is an assumption of a rigidity-dependent acceleration in sources. In terms of maximum acceleration energy it may be formulated as $E_{\max}^{\text{acc}} = ZE_0$, where E_0 is a universal energy to be determined from data, and Z is a nucleus charge number. These three assumptions complete the definition of the model.

The main approach of this work is as follows. We determine first the maximum acceleration energy for protons, $E_p^{\max} = E_0$. For this we calculate the extragalactic diffuse proton flux assuming the power-law

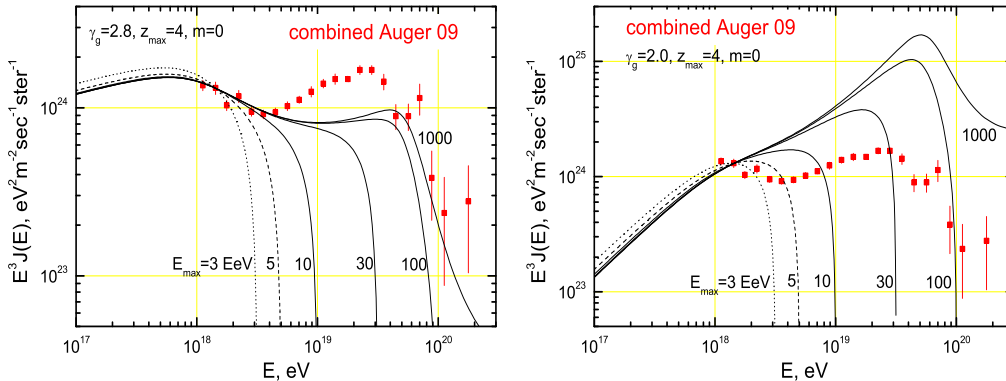


Figure 4: Comparison of calculated proton spectra with the combined Auger spectrum for different E_p^{\max} . Extreme cases $\gamma_g = 2.8$ and 2.0 are shown in the left and right panels, respectively. The allowed E_{\max} corresponds to curves lying below experimental points at $E \sim 4$ EeV, from which nuclei start dominating.

generation spectrum $Q_g(E) \propto E^{-\gamma_g}$ with $E_{\max} = E_0$ and normalizing the calculated flux by the Auger flux at $(1 - 3)$ EeV. Varying γ_g in the range $2.0 - 2.8$, we search for a maximum value of E_0 allowed by the Auger mass composition and energy spectrum. Increasing E_0 beyond this limit one comes to a contradiction either with mass composition or with energy spectrum in Fig. 3.

The results are presented in Fig. 4. In calculations we use a homogeneous distribution of sources without cosmological evolution (evolution parameter $m = 0$) and with maximal redshift $z_{\max} = 4$. As a criterion of contradiction we choose an excess of calculated proton flux at energy $(4 - 5)$ EeV, where Auger data show the dominance of nuclei. The contradiction has different character for different values of γ_g .

For steep source generation functions with $\gamma_g \simeq 2.6 - 2.7$ the shape and flux of the Auger spectrum may be described by $E_p^{\max} \sim 10^{20} - 10^{21}$ eV; the contradiction occurs only in data on mass composition. The extreme case, given by $\gamma_g = 2.8$, is displayed in the left panel of Fig. 4. In fact all curves with $E_{\max} \geq 10$ EeV are below the data points at $E > 5$ EeV and hence compatible with Auger energy spectrum. However, these curves are excluded by prediction of the pure proton composition at $E \sim (4 - 5)$ EeV, i.e. due to contradiction in mass composition in a very narrow energy range (see Fig. 4).

For flat generation spectra the contradiction is very pronounced: the predicted total proton flux exceeds the observed one. It can be seen in the right panel of Fig. 4 for another extreme case, $\gamma_g = 2.0$: for $E_{\max} = 5$ EeV the calculated proton flux exceeds the observed one at $E \approx 2$ EeV.

We conclude with some redundancy that $E_p^{\max} \sim (4 - 10)$ EeV holds for all generation indices in the range $2.0 - 2.8$. The maximum energy for Iron nuclei is $Z = 26$ times higher and does not exceed $E_{\text{Fe}}^{\max} \sim (100 - 300)$ EeV.

In the end of this section we discuss our main assumption that the particles observed at energy $(1 - 3)$ EeV are protons. Within experimental uncertainties they can be Helium. Does it exclude our conclusion about low E_{\max} ?

Our calculations with He nuclei show that, in contrast to protons, we cannot fit well the three spectral points at energies $(1 - 3)$ EeV with good enough accuracy. The best, though not good, fit is given by $\gamma_g = 2.8$ and $E_{\text{He}}^{\max} = 4$ EeV. However, even this case has an additional difficulty: the spectrum of Fe nuclei is too steep and cannot explain the highest energy flux measured by Auger.

3. The Auger total energy spectrum

In Fig. 5 we plot the calculated total UHECR spectrum in the 'disappointing model', using $\gamma_g = 2.3$, which might be the case for acceleration by relativistic shocks. The proton spectrum is calculated here in a diffusive model, the more realistic one for energies below 1 EeV. We assume the turbulent magnetic field with basic scales $(B_c, l_c) = (1 \text{ nG}, 1 \text{ Mpc})$, the distance between sources $d \sim 40 \text{ Mpc}$ and the Kolmogorov

diffusion coefficient (for notation and method of calculation see [24, 25]). The analysis of proton maximum energy of acceleration (see left panel of Fig. 5) gives $E_0 = E_p^{\max} = 4$ EeV, in a rough agreement with the analysis made for homogeneous distribution of sources. In fact this set of parameters gives the lowest E_0 allowed by Auger data, because a prediction for the maximum energy of Iron nuclei is 100 EeV, while in Auger one event with energy close to 200 EeV was already observed. However, varying parameters, in particular increasing γ_g , it is easy to increase E_0 to (5 – 6) EeV, and even 10 EeV cannot be excluded.

The account for diffusion in extragalactic magnetic fields provides a flattening of the proton spectrum at $E \lesssim 1$ EeV, seen in Fig. 5 as a 'diffusive cutoff', because flux $J(E)$ is multiplied by E^3 . The 'diffusive cutoff' provides a transition from the steep galactic spectrum, most probably composed of Iron, to the flat spectrum of extragalactic protons.

The spectrum of nuclei in Fig. 5 is obtained by subtraction procedure first suggested in [26]. We subtract the above-calculated proton spectrum from the total Auger spectrum. The resultant flux is plotted in the right panel of Fig. 5 as a sum of different nuclei species. In the mixed composition model [27, 28] it looks quite possible to fit the obtained nuclei spectrum by allowing for arbitrary fractions of primary nuclei in sources.

The basic feature of the Auger mass composition, the progressively heavier composition with energy increasing, is guaranteed in our model by the rigidity-dependent maximum energy of acceleration: at energy higher than ZE_p^{\max} nuclei with charge $Z' < Z$ disappear, while heavier nuclei with larger Z survive. Starting from $E_p^{\max} \sim (4 - 10)$ EeV, the higher energies are accessible only for nuclei with progressively larger values of Z . In particular, the maximum observed energy must correspond to Iron nuclei, which can reach $E \sim (100 - 300)$ EeV. In the next paper we plan to perform detailed calculations for diffusive propagation of nuclei with sources located in vertices of a cubic grid similar to [29, 25].

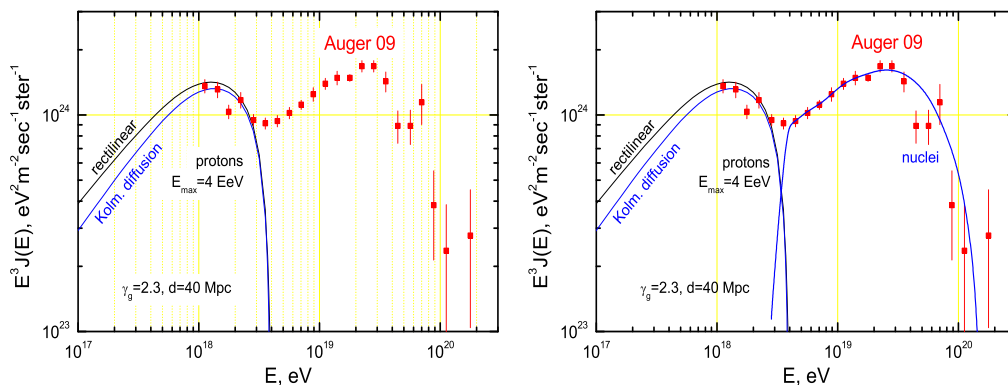


Figure 5: *Left panel:* Comparison of calculated proton spectra with the combined Auger spectrum for $\gamma_g = 2.3$ and diffusive proton propagation (see text for details). The cutoff at $E_p^{\max} = 4$ EeV is needed to avoid the contradiction with data at $E > 3$ EeV. *Right panel:* Total UHECR spectrum in 'disappointing model' in comparison with the combined Auger spectrum. Spectrum of protons is taken from the left panel. The spectrum of nuclei is obtained by subtraction procedure as described in the text.

As a next step to exact calculations we consider a two-component model, with only protons and Iron nuclei being produced in sources. The generation index $\gamma_g = 2.0$ and the maximum acceleration energy $E_{\max} = 4Z$ EeV. The proton spectrum is calculated as above and the primary Iron nuclei spectrum is calculated as in [30, 31] for homogeneous distribution of sources. The spectra are presented in the left panel of Fig. 6. One may notice that the calculated spectrum of Iron describes well the cutoff in the Auger spectrum, which we failed to explain in many models of GZK cutoff. This steepening is caused by the photo-disintegration of Iron nuclei. The sharp acceleration cutoff at $E_{\text{Fe}}^{\max} = ZE_p^{\max}$ is not shown in this figure.

To agree with Auger-observed mass composition, the Iron spectrum in Fig. 6 must have a low-energy cutoff at $E \lesssim (20 - 30)$ EeV. Most naturally it is produced as a 'diffusive cutoff' which appears in models with lattice-located sources due to *magnetic horizon*.

The magnetic horizon arises automatically in solutions of diffusion equations, e.g. in the Syrovatsky solution [32], due to the Green function

$$G(E, \vec{r}; E_g, \vec{r}_g) \propto \exp \left[-\frac{(\vec{r} - \vec{r}_g)^2}{4\lambda(E, E_g)} \right], \quad (1)$$

where \vec{r} and \vec{r}_g are positions of an observer and a source, respectively, and λ is given below by Eq. (2). Energies of primary Iron nuclei practically do not change during the lifetime of photo-disintegration τ , and λ can be given as

$$\lambda(E, \tau) = \int_0^\tau dt D(E, t) \approx D(E) \tau, \quad (2)$$

where $D(E)$ is the diffusion coefficient at energy E . Thus, radius of the horizon and a condition when it cuts the spectrum off are given by

$$r_{\text{hor}}^2 = 4 D(E) \tau \leq d^2, \quad (3)$$

where d is the lattice constant (length), which is of order of distance to the nearest source.

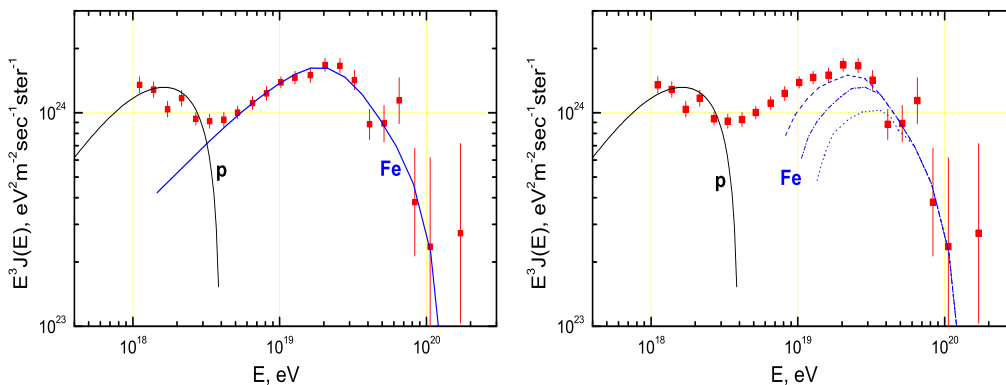


Figure 6: *Left panel:* The energy spectrum in two-component model with protons and Iron nuclei with $\gamma_g = 2.0$ and $E_{\text{max}} = 4Z$ EeV. The Iron nuclei spectrum is calculated for homogeneous distribution of the sources. *Right panel:* As in the left panel, but with the 'diffusion cutoff' introduced for three different sets of parameters B_c, l_c, d . The gap between 2 EeV and E_{cut} (beginning of 'diffusive cutoff') is expected to be filled by intermediate nuclei.

For description of the diffusion we use as in [32] the magnetic field configuration $(B_c, l_c) = (1 \text{ nG}, 1 \text{ Mpc})$, with the diffusion coefficient

$$D(E) = D_0 \left(\frac{E}{E_c} \right)^n, \quad \text{and} \quad D_0 = \frac{1}{3} c l_c, \quad (4)$$

where $n = 1/3$ at $E < E_c$, and $n = 2$ at $E \gg E_c$, and

$$E_c = Z e B_c l_c = 24 \times \frac{Z}{26} \times \frac{B_c}{1 \text{ nG}} \times \frac{l_c}{1 \text{ Mpc}} \text{ EeV}. \quad (5)$$

From Eqs. (3) - (4) one obtains for the energy of cutoff E_{cut} :

$$\left(\frac{E_{\text{cut}}}{E_c} \right)^n = \frac{3d^2}{4c\tau l_c} = 2.2 \times \left(\frac{d}{30 \text{ Mpc}} \right)^2 \times \left(\frac{10^9 \text{ yr}}{\tau} \right). \quad (6)$$

For $20 \lesssim d \lesssim 50 \text{ Mpc}$ and $\tau \sim (0.1 - 1) \times 10^9 \text{ yr}$ [30, 31], we finally get

$$E_{\text{cut}} \sim E_c = 24 \times \frac{Z}{26} \times \frac{B_c}{1 \text{ nG}} \times \frac{l_c}{1 \text{ Mpc}} \text{ EeV}. \quad (7)$$

For the natural choice of parameters B_c, l_c, d the beginning of the 'diffusive cutoff' can start at $E_{\text{cut}} \sim E_c$. When E decreases, the $D(E)$ decreases too, and the horizon becomes less than distance to a nearby source. Still particles can arrive from there, being however stronger suppressed by the exponent in Eq. (1). Cutoff is expected to be sharp, but this statement expects a validation by numerical calculations.

In the right panel of Fig. 6 we introduce in the Iron spectrum the low-energy 'diffusive cutoff' for three different sets of parameters B_c, l_c, d . The beginning of this cutoff E_c for Iron nuclei is $Z = 26$ times higher than for protons, i.e. $E_c \approx 2.6 \times 10^{19}$ eV, which has a reasonable physical meaning. The gap between 2 EeV and 26 EeV is expected to be filled by intermediate nuclei. To provide a smooth RMS curve seen in the Auger data (Fig. 3) in this energy interval, we have many free parameters at our disposal in the form of arbitrary fractions of nuclei accelerated in a source. We plan to perform the detailed calculations in the future work.

4. Predictions and uncertainties

The predictions of our model are very disappointing for the future detectors.

The maximum acceleration energy $E_{\text{max}} \sim (100 - 300)$ EeV for Iron nuclei implies the energy per nucleon $E_p < E_{\text{max}}/A \sim (2 - 5)$ EeV, well below the GZK cutoff for epochs with $z \lesssim 15$. Therefore, practically no cosmogenic neutrinos can be produced in collisions of protons and nuclei with CMBR photons. However neutrinos with $E_\nu \lesssim 1 \times 10^{17}$ eV can be generated in collisions of protons and nuclei with Extragalactic Background Light (EBL) photons; we will refer to these neutrinos as the EBL-produced ones. The main mechanism of their generation in our model is the decay of pions photo-produced by primary EeV protons on EBL. The EBL-produced neutrinos are also generated by nuclei after their photo-disintegration to nucleons. This mechanism provides a lower neutrino flux, because the secondary protons in our model are subdominant in comparison with the primary ones. Finally, an additional neutrino flux appears at further lower energies due to decays of neutrons, the fragments of photo-disintegrated nuclei. The EBL-produced neutrino fluxes have been calculated under different assumptions in many papers, see e.g. [33, 34, 35, 36, 37, 38].

For our case it was convenient to use the calculations of [37], where neutrino fluxes were given separately for production on CMBR, EBL and due to neutron decays. We used these calculations to estimate the upper limit for the EBL-produced neutrinos in our model. We found it to be 6 times below the upper limit which is expected to be obtained by IceCube after 5 years of observations [39]. The neutrino flux from neutron decays is less than this flux by two orders of magnitude.

Correlation with UHECR sources also is absent due to deflection of nuclei in the galactic magnetic fields. The lack of correlation in the model is strengthened by dependence of the maximum energy on Z .

The signatures of the 'disappointing model' for the Auger detector are the mass-energy relation, already seen in the elongation curve $X_{\text{max}}(E)$, and transition from galactic to extragalactic cosmic rays below the characteristic energy $E_c \sim 1$ EeV.

There are some uncertainties in the model presented above. The most important one relates to estimates of E_p^{max} . It is determined by the lowest energy where Auger data are inconsistent with proton composition (the 6th low-energy bin of the Auger data in Fig. 3). If this energy increases, E_p^{max} increases, too. The model collapses when allowed E_p^{max} reaches e.g. (50 - 100) EeV. Another case is given by the mass composition being heavy starting from 1 EeV. The cosmological evolution of sources are not included in our calculations. Since this effect slightly decreases E_p^{max} , it is not needed to be taken into account. It is also possible that the EeV protons detected by Auger are secondary ones, i.e. those produced in photo-dissociation of primary nuclei in collisions with CMBR and extragalactic IR/UV photons. However, it was demonstrated in [30, 31] that the flux of secondary protons in the EeV range is always smaller than the flux of parent primary nuclei. According to [40] it is considerably smaller than the sum of primary and secondary nuclei fluxes.

5. Discussions and conclusions

The suggested model is aimed at explanation of the observational data of the Auger detector only. The crucial for the model feature is (i) the proton composition in the energy range (1 - 3) EeV, considered in our

paper as an assumption. Two additional assumptions are (ii) the extragalactic origin of the observed protons and (iii) their acceleration by the rigidity dependent mechanism with $E_{\max} = ZE_0$, where universal energy E_0 is the same for all nuclei. The upper limit on E_0 (maximum acceleration energy for protons) is obtained by calculating the proton spectrum at higher energies using the generation index γ_g and normalizing flux at (1 – 3) EeV by the Auger data. The cutoff of the proton spectrum at E_0 provides an agreement between the Auger flux and mass composition at higher energies. The calculations are performed for homogeneously distributed UHECR sources with cosmological evolution being neglected. Maximum redshift of sources is $z_{\max} = 4$; indices of source power-law generation functions γ_g vary in the wide range from 2.0 to 2.8. The obtained upper limit on E_0 is (4 – 10) EeV. The maximum predicted energy corresponds to Iron and equals to (100 – 300) EeV. The maximum energy per nucleon is only (2 – 5) EeV, and pion photo-production processes on CMBR are practically absent. Therefore, the GZK cutoff in the UHECR spectrum and the production of cosmogenic neutrinos are absent, too. The observed cutoff of the spectrum is provided by the nuclei photo-disintegration and is strengthened by the acceleration cutoff.

The rigidity-dependent E_{\max} provides the energy-dependent mass composition: at energy higher than ZE_0 nuclei with charge Z disappear, while heavier ones, with larger Z , survive. It agrees qualitatively with the Auger observations. This feature disfavors the correlation with UHECR sources at highest energies: at 100 EeV Iron nuclei dominate in the spectrum and their deflection in the galactic magnetic fields prevents the correlation with possible sources.

There are two signatures of this model for Auger data. The realistic one is the transition from galactic to extragalactic cosmic rays. This transition occurs due to intersection of the flat extragalactic proton spectrum with the steep one of galactic Iron nuclei. The flat spectrum of protons below 1 EeV appears due to diffusion of protons in extragalactic magnetic fields [41, 42]. The transition below 1 EeV combined with the nuclei composition above (3 – 5) EeV is a strong signature of the model under discussion.

The second signature is the energy-dependent mass composition, getting progressively heavier with energy increasing. The indication to this feature is already seen in the Auger data.

Is there any alternative explanation of the EeV protons in the Auger data?

The EeV protons could have galactic origin, though it contradicts the Standard Model for the galactic cosmic rays (see e.g. [43]), where maximum acceleration energy, $E_{\max}^{\text{acc}} \approx 1 \times 10^{17}$ eV, is attained by Iron nuclei. However, one may assume an additional high-energy proton component of the galactic cosmic rays extending up to (2 – 3) EeV. The usual argument with anisotropy could be bypassed considering a case suggested in [44]. GRB could occur in our Galaxy $10^6 - 10^7$ years ago producing high energy protons by inner-shocks acceleration. The protons propagate in the mode of non-stationary diffusion, so that most of particles have already escaped from Galaxy and now only the tail of retarded particles with a reduced anisotropy is observed. In this model the transition from galactic to extragalactic cosmic rays occurs at ankle, which is clearly seen in the Auger data. This case differs from the “standard” ankle model, where transition occurs from galactic Iron to extragalactic protons; it needs a more detailed investigation.

Another similar example is given by the model [45], where all observed cosmic rays have galactic origin, and the Galactic GRBs are considered as sources. The primaries are assumed to be protons and Iron nuclei, which dominate at low and highest energies, respectively.

In conclusion, we face at present the most serious disagreement in the observational data of the two biggest experiments in UHECR.

HiRes observes signatures of proton propagation through CMBR in the form of the pair-production dip and GZK cutoff, and these observations are well confirmed by direct measurements of the proton-dominated mass composition. These observations predict a detectable accompanying UHE neutrino flux. The neutrino flux predicted in proton-dominated models [38] may be registered by the future JEM-EUSO [46] in the case of large E_{\max} and strong cosmological evolution of the sources. This detector can also observe the nearby UHECR sources using protons with energies up to 100 EeV and above.

Auger clearly observes the high-energy steepening of the spectrum, but its position and shape are rather different from the prediction of the GZK cutoff. The mass composition at $E \gtrsim 4$ EeV shows the dominance of nuclei becoming progressively heavier with energy increasing and probably reaching the pure Iron composition at $E \approx 35$ EeV. The Auger data allow the most conservative explanation in terms of low maximum-energy of acceleration, based on the observation of the EeV protons. It seriously ameliorates the

problem of acceleration in astrophysical sources, diminishing the maximum energy down to (100 – 300) EeV for Iron nuclei. This conservative and disappointing scenario can be confirmed by transition from galactic to extragalactic cosmic rays below 1 EeV, by absence of cosmogenic neutrinos and by agreement with elongation rate calculated in this model.

6. Acknowledgments

This work was presented at JEM-EUSO meeting on July 19-20 2009 and we are grateful to Alan Watson for encouraging us to write a paper and for valuable advices. We are very thankful to all participants of the SOCoR Workshop in Trondheim on June 15-18 2009, where the new Auger and HiRes data were presented and discussed, and a real brain attack on the problem was undertaken. We are grateful to Michael Kachelrieß, the main organizer of this remarkable workshop. We are also grateful to anonymous Referee for useful remarks. The work of A.Gazizov was supported in part by contract with Gran Sasso Center for Astroparticle Physics (CFA) funded by European Union and Regione Abruzzo under the contract P.O. FSE Abruzzo 2007-2013, Ob. CRO.

References

- [1] R. U. Abbasi, et al., Observation of the GZK cutoff by the HiRes experiment, *Phys. Rev. Lett.* 100 (2008) 101101. [arXiv:astro-ph/0703099](#), [doi:10.1103/PhysRevLett.100.101101](#).
- [2] J. Abraham, et al., Observation of the suppression of the flux of cosmic rays above 4×10^{19} eV, *Phys. Rev. Lett.* 101 (2008) 061101. [arXiv:0806.4302](#), [doi:10.1103/PhysRevLett.101.061101](#).
- [3] K. Greisen, End to the cosmic ray spectrum?, *Phys. Rev. Lett.* 16 (1966) 748–750. [doi:10.1103/PhysRevLett.16.748](#).
- [4] G. T. Zatsepin, V. A. Kuzmin, Upper limit of the spectrum of cosmic rays, *JETP Lett.* 4 (1966) 78–80.
- [5] V. S. Berezhinsky, S. I. Grigor’eva, A Bump in the ultrahigh-energy cosmic ray spectrum, *Astron. Astrophys.* 199 (1988) 1–12.
- [6] V. Berezhinsky, A. Z. Gazizov, S. I. Grigorieva, On astrophysical solution to ultra high energy cosmic rays, *Phys. Rev. D* 74 (2006) 043005. [arXiv:hep-ph/0204357](#), [doi:10.1103/PhysRevD.74.043005](#).
- [7] R. Aloisio, et al., A dip in the UHECR spectrum and the transition from galactic to extragalactic cosmic rays, *Astropart. Phys.* 27 (2007) 76–91. [arXiv:astro-ph/0608219](#), [doi:10.1016/j.astropartphys.2006.09.004](#).
- [8] V. Berezhinsky, A. Z. Gazizov, S. I. Grigorieva, Signatures of AGN model for UHECR, [arXiv:astro-ph/0210095](#) (2002).
- [9] V. Berezhinsky, A. Z. Gazizov, S. I. Grigorieva, Dip in UHECR spectrum as signature of proton interaction with CMB, *Phys. Lett. B* 612 (2005) 147–153. [arXiv:astro-ph/0502550](#), [doi:10.1016/j.physletb.2005.02.058](#).
- [10] P. Sokolsky, Results from HiRes, in: Searching for the Origins of Cosmic Rays (SOCoR 2009), <http://web.phys.ntnu.no/~mika/programme.html>, Department of Physics, NTNU Trondheim, Norway, 2009.
- [11] P. Sokolsky, Final Results from the High Resolution Fly’s Eye (HiRes) Experiment, [arXiv:1010.2690](#).
- [12] D. Ikeda, Results from the telescope array experiment (invited), in: 22nd European Cosmic Ray Symposium, ECRS 2010, University of Turku, Finland, Faculty of Education, University of Turku, 2010.
- [13] G. B. Thomson, Results from the Telescope Array Experiment, [arXiv:1010.5528](#).
- [14] S. Ostapchenko, Non-linear screening effects in high energy hadronic interactions, *Phys. Rev. D* 74 (2006) 014026. [arXiv:hep-ph/0505259](#), [doi:10.1103/PhysRevD.74.014026](#).
- [15] P. Sokolsky, New results from HIRES and Telescope Arrays, in: The XXIst Rencontres de Blois: Windows on the Universe, http://blois.in2p3.fr/2009/plenary_sessions.html, June 2009.
- [16] R. U. Abbasi, et al., Indications of Proton-Dominated Cosmic Ray Composition above 1.6 EeV, *Phys. Rev. Lett.* 104 (2010) 161101. [arXiv:0910.4184](#), [doi:10.1103/PhysRevLett.104.161101](#).
- [17] M. Unger, Study of the Cosmic Ray Composition with the PAO, in: Searching for the Origins of Cosmic Rays, <http://web.phys.ntnu.no/~mika/programme.html>, SOCoR 2009, Department of Physics, NTNU Trondheim, Norway, 2009.
- [18] J. Abraham, et al., Measurement of the Depth of Maximum of Extensive Air Showers above 10^{18} eV, *Phys. Rev. Lett.* 104 (2010) 091101. [arXiv:1002.0699](#), [doi:10.1103/PhysRevLett.104.091101](#).
- [19] J. A. Bellido, Measurement of the average depth of shower maximum and its fluctuations with the Pierre Auger Observatory, in: Proceedings of the 31st ICRC, ŁÓDŹ 2009, University of Łódź with Andrzej Soltan Institute for Nuclear Studies, 2009.
- [20] R. Aloisio, V. Berezhinsky, P. Blasi, S. Ostapchenko, Signatures of the transition from galactic to extragalactic cosmic rays, *Phys. Rev. D* 77 (2008) 025007. [arXiv:0706.2834](#), [doi:10.1103/PhysRevD.77.025007](#).
- [21] V. Berezhinsky, The origin of ultra high energy cosmic rays, in: invited talk at 15th International Cosmic Ray Conference, Plovdiv, Bulgaria, Vol. 10, 1977, pp. 84–107.
- [22] K. Mannheim, R. J. Protheroe, J. P. Rachen, On the cosmic ray bound for models of extragalactic neutrino production, *Phys. Rev. D* 63 (2001) 023003. [arXiv:astro-ph/9812398](#), [doi:10.1103/PhysRevD.63.023003](#).
- [23] A. M. Atoyan, C. D. Dermer, Neutral beams from blazar jets, *Astrophys. J.* 586 (2003) 79–96. [arXiv:astro-ph/0209231](#), [doi:10.1086/346261](#).

- [24] V. Berezhinsky, A. Z. Gazizov, Diffusion of Cosmic Rays in Expanding Universe. (I), *Astrophys. J.* 643 (2006) 8–13. [arXiv:astro-ph/0512090](#), [doi:10.1086/502626](#).
- [25] R. Aloisio, V. Berezhinsky, A. Gazizov, Superluminal problem in diffusion of relativistic particles and its phenomenological solution, *Astrophys. J.* 693 (2009) 1275–1282. [arXiv:0805.1867](#), [doi:10.1088/0004-637X/693/2/1275](#).
- [26] V. S. Berezhinsky, S. I. Grigorieva, B. I. Hnatyk, Extragalactic UHE proton spectrum and prediction for iron-nuclei flux at $10^{*}8$ -GeV to $10^{*}9$ -GeV, *Astropart. Phys.* 21 (2004) 617–625. [arXiv:astro-ph/0403477](#), [doi:10.1016/j.astropartphys.2004.06.004](#).
- [27] D. Allard, E. Parizot, E. Khan, S. Goriely, A. V. Olinto, UHE nuclei propagation and the interpretation of the ankle in the cosmic-ray spectrum, *Astron. Astrophys.* 443 (2005) L29–L32. [arXiv:astro-ph/0505566](#).
- [28] D. Allard, E. Parizot, A. V. Olinto, On the transition from Galactic to extragalactic cosmic-rays: spectral and composition features from two opposite scenarios, *Astropart. Phys.* 27 (2007) 61–75. [arXiv:astro-ph/0512345](#), [doi:10.1016/j.astropartphys.2006.09.006](#).
- [29] V. Berezhinsky, A. Z. Gazizov, Diffusion of cosmic rays in the expanding universe. II: Energy spectra of ultra-high energy cosmic rays, *Astrophys. J.* 669 (2007) 684–691. [arXiv:astro-ph/0702102](#), [doi:10.1086/520498](#).
- [30] R. Aloisio, V. Berezhinsky, S. Grigorieva, Analytic calculations of the spectra of ultra-high energy cosmic ray nuclei. I. The case of CMB radiation, [arXiv:0802.4452](#).
- [31] R. Aloisio, V. Berezhinsky, S. Grigorieva, Analytic calculations of the spectra of ultra high energy cosmic ray nuclei. II. The general case of background radiation, [arXiv:1006.2484](#).
- [32] R. Aloisio, V. Berezhinsky, Diffusive propagation of UHECR and the propagation theorem, *Astrophys. J.* 612 (2004) 900–913. [arXiv:astro-ph/0403095](#), [doi:10.1086/421869](#).
- [33] R. Engel, D. Seckel, T. Stanev, Neutrinos from propagation of ultra-high energy protons, *Phys. Rev. D* 64 (2001) 093010. [arXiv:astro-ph/0101216](#), [doi:10.1103/PhysRevD.64.093010](#).
- [34] T. Stanev, Ultrahigh Energy Cosmic Rays and Neutrinos, *Nucl. Instrum. Meth.* A588 (2008) 215–220. [arXiv:0711.1872](#), [doi:10.1016/j.nima.2008.01.043](#).
- [35] M. Ave, N. Busca, A. V. Olinto, A. A. Watson, T. Yamamoto, Cosmogenic neutrinos from ultra-high energy nuclei, *Astropart. Phys.* 23 (2005) 19–29. [arXiv:astro-ph/0409316](#), [doi:10.1016/j.astropartphys.2004.11.001](#).
- [36] D. Hooper, A. Taylor, S. Sarkar, The impact of heavy nuclei on the cosmogenic neutrino flux, *Astropart. Phys.* 23 (2005) 11–17. [arXiv:astro-ph/0407618](#), [doi:10.1016/j.astropartphys.2004.11.002](#).
- [37] K. Kotera, D. Allard, A. V. Olinto, Cosmogenic Neutrinos: parameter space and detectability from PeV to ZeV, *JCAP* 1010 (2010) 013. [arXiv:1009.1382](#), [doi:10.1088/1475-7516/2010/10/013](#).
- [38] V. Berezhinsky, A. Gazizov, M. Kachelriess, S. Ostapchenko, Fermi-LAT restrictions on UHECRs and cosmogenic neutrinos, [arXiv:1003.1496](#).
- [39] J. Ahrens, et al., Sensitivity of the IceCube detector to astrophysical sources of high energy muon neutrinos, *Astropart. Phys.* 20 (2004) 507–532. [arXiv:astro-ph/0305196](#), [doi:10.1016/j.astropartphys.2003.09.003](#).
- [40] D. Allard, N. G. Busca, G. Decerprit, A. V. Olinto, E. Parizot, Implications of the cosmic ray spectrum for the mass composition at the highest energies, *JCAP* 0810 (2008) 033. [arXiv:0805.4779](#), [doi:10.1088/1475-7516/2008/10/033](#).
- [41] M. Lemoine, Extra-galactic magnetic fields and the second knee in the cosmic-ray spectrum, *Phys. Rev. D* 71 (2005) 083007. [arXiv:astro-ph/0411173](#), [doi:10.1103/PhysRevD.71.083007](#).
- [42] R. Aloisio, V. S. Berezhinsky, Anti-GZK effect in UHECR diffusive propagation, *Astrophys. J.* 625 (2005) 249–255. [arXiv:astro-ph/0412578](#), [doi:10.1086/429615](#).
- [43] E. G. Berezhko, H. J. Völk, Spectrum of cosmic rays, produced in supernova remnants, *Astrophys. J.* 661 (2007) L175–L177. [arXiv:0704.1715](#).
- [44] S. D. Wick, C. D. Dermer, A. Atoyan, High-energy cosmic rays from gamma-ray bursts, *Astropart. Phys.* 21 (2004) 125–148. [arXiv:astro-ph/0310667](#), [doi:10.1016/j.astropartphys.2003.12.008](#).
- [45] A. Calvez, A. Kusenko, S. Nagataki, Role of Galactic sources and magnetic fields in forming the observed energy-dependent composition of ultrahigh-energy cosmic rays, *Phys. Rev. Lett.* 105 (2010) 091101. [arXiv:1004.2535](#), [doi:10.1103/PhysRevLett.105.091101](#).
- [46] Y. Takahashi, The JEM-EUSO mission, *New J. Phys.* 11 (2009) 065009. [doi:10.1088/1367-2630/11/6/065009](#).